ARTICLES

On the Multielectron Dissociative Ionization of Some Cyclic Aromatic Molecules Induced by Strong Laser Fields

P. Tzallas,[†] C. Kosmidis,[*,†] K. W. D. Ledingham,[‡] R. P. Singhal,[‡] T. McCanny,[‡] P. Graham,[‡] S. M. Hankin,[‡] P. F. Taday,[§] and A. J. Langley[§]

Atomic and Molecular Physics Laboratory, Department of Physics, P.O. Box 1186, University of Ioannina, GR-451 10 Ioannina, Greece, Department of Physics and Astronomy, University of Glasgow, Glasgow G12 8QQ, Scotland, U.K., and Central Laser Facility, Rutherford Appleton Laboratory, Didcot, Oxon, OX11 0QX, England, U.K.

Received: March 23, 2000; In Final Form: September 7, 2000

The interaction of strong laser fields (4×10^{16} W/cm^2) with cyclic aromatic molecules (furan, pyrrole, pyridine, and pyrazine) has been studied at $\lambda = 790$ nm. The fragmentation processes of multiply charged transient molecular ions were analyzed by means of a time-of-flight (TOF) spectrometer. Most ion peaks consisted of one broad and one sharp component. From the analysis of the peak profiles the kinetic energies of the molecular and atomic fragment ions have bean measured. On the basis of these energy values and the estimated charge separation distances, it is concluded that, for furan, it is probable that Coulomb explosion takes place in multiple charged parent ions with deformed molecular structure. The doubly charged parent ions of furan and pyrrole fragments through charge separation processes. At higher charged transient parent ions the fragmentation proceeds through direct (instantaneous) process. Moreover, there is evidence that, at least for furan, the ionization process takes place via a direct field ionization mechanism. Pyridine and pyrazine multiple charged ions seem to follow different dissociation routes. The abundance ratios C^+/A^+ (A = N, O) for the singly charged atoms were found to be equal to the stoichiometric ratio for all the molecules studied, while a divergence has been observed for the $C^{2,3+}/A^{2,3+}$ (A = N, O) ratios.

Introduction

Molecular ionization and dissociation by strong laser radiation has been the subject of increasing interest in recent years.[1−10] Within this field, the interaction with polyatomic molecules has proven to be of particular interest.

The first questions concerned the mechanism, which is responsible for molecular ionization. As expected this is strongly related to the laser intensity. A field ionization mechanism seems to be dominant for some polyatomic molecules even for the Keldysh parameter[11] γ greater than 1. DeWitt and Levis[12,13] have shown that molecular systems with extended delocalization can pass from the MPI to the field ionization regime for values $\gamma \sim 3$. The same group[14−16] and Castellejo et al.[17] have studied the influence of molecular structure on the ionization/dissociation processes in polyatomic molecules.

Using laser light of different pulse duration (nanosecond−femtosecond), it has been shown that for laser intensities about 3×10^{11} W/cm^2 the irradiation with femtosecond pulses leads to intact molecular ion production which is absent in the nsec laser-induced mass spectra.[18] This observation has been verified at $I \sim 10^{13}$ W/cm^2 for some other molecules, too,[19−21] and the potential of femtosecond laser mass spectrometry for analytical purposes has been discussed.[22,23]

The progress in femtosecond laser technology has made available tabletop laser systems with higher intensities. The interaction of some polyatomic molecules with laser intensities of $10^{15}-10^{16}$ W/cm^2 has led to the observation of multiply charged parent ions.[24,25] Recently, the relation between the molecular and intact doubly charged polyatomic ions has been explored[26] and it has been observed that, regardless of the appearance in the mass spectra of the doubly charged parent ion, strong multiply charged atomic fragments were present in the spectra.

In this work the generation of multiply charged atomic ions induced by strong laser fields ($\sim 4 \times 10^{16}$ W/cm^2) is studied by means of a time-of-flight (TOF) mass spectrometry technique. Aromatic heterocyclic molecules (furan, pyrrole, pyridine, pyrazine) were chosen for investigation. Furan and pyrrole have a five member ring, while the other molecules have a six-member ring. In the former molecules different heteroatoms are participating in the aromatic ring (O, N atoms, respectively), while in pyridine and pyrazine there is a different number of (1 and 2, respectively) of the same heteroatom (nitrogen).

The aim of these measurements is to understand the dissociation processes in multiple charged ions. The atomic fragment ions could be produced through a direct (instantaneous) multi-

* Author for correspondence. E-mail: kkosmid@cc.uoi.gr. Fax: 0030-651-98695.
[†] Department of Physics.
[‡] Department of Physics and Astronomy.
[§] Central Laser Facility.

10.1021/jp001096m CCC: $20.00
Published on Web 12/16/2000

fragmentation explosion of a highly charged (transient) parent molecular ion[7]

$$[P^{n+}] \rightarrow A^{n_1+} + B^{n_2+} + ... + C^{n_i} + \text{kinetic energy}, \quad (n = n_1 + n_2 + ... + n_i)$$

or via a sequential molecular dissociation process

$$[P^{m+}] \rightarrow [F_1^{m_1+}] + [F_2^{m_2+}] + ... + [F_k^{m_k+}] + \text{kinetic energy}, \quad (m = m_1 + m_2 + ... + m_k)$$

$$[F_k^{m_k+}] \rightarrow A^{m_1+} + B^{m_2+} + ... + C^{m_i+} + \text{kinetic energy}, \quad (m_k = m_1 + m_2 + ... + m_i)$$

The contribution to atomic ion production of the ionization of an F_k neutral fragment (which generally could produce an atomic or a molecular fragment) is not considered because the pulse duration (75 fs) of the laser used is shorter than the typical time scale of the molecular dissociation processes.

Experimental Details

The experimental set up used is described in detail elsewhere.[27] Briefly, the time-of-flight (TOF) mass spectrometer is of conventional linear arrangement with ion optics based on a Wiley−McLaren design.

The samples were admitted effusively from the inlet system to the vacuum chamber via a needle valve after passing through a hole ($2R = 1$ mm) in the repeller electrode of the TOF. The ion optics in the extraction region consists of three circular plates of diameter 25 mm separated by 5 mm. One of these is the repeller electrode mentioned above and the other two have circular apertures of diameter 10 mm. The repeller electrode was operated at 2.5 kV while the two apertured electrodes were operated at 2.1 and 0 kV, respectively.

The laser system is based on a Ti:S oscillator pumped by a Spectra-Physics Millenia laser[28] and using the Chirped Pulse Amplification (CPA) technique. It produces output pulses at 790 nm, with a 75 fs duration and a pulse energy of ~10mJ with a repetition rate of 10 Hz. Controlled attenuation of the beam energy was achieved by a variable neutral density filter and the corresponding energies were measured in front of the vacuum chamber with a joulemeter. The laser beam was focused at about 4 mm from the repeller using a concave mirror with a focal length of 5 cm. Optimum spatial ionizing conditions were achieved using a *xyz* vernier controlled mechanism coupled to the focusing mirror. The mass resolution was typically 200 at 100D.

A Thorn EMI electron multiplier coupled to a Lecroy 9304 digital oscilloscope recorded the mass spectra, typically averaging over hundreds of laser shots for each spectrum.

Of particular importance is the accurate determination of the laser intensity at the focal point. The intensity values in this work have been estimated by dividing the corrected pulse energy (for the losses caused by the optical components used (entrance window and focusing mirror)) by the theoretical value of the focal area. The latter could introduce some errors in laser intensity estimations. To check it, Ar gas has been introduced in the chamber and the mass spectra have been recorded at the highest available laser intensity. In the recorded mass spectra the Ar^{7+} ion peak has been clearly observed, while the Ar^{8+} ion is almost absent. The threshold intensities for the appearance of Ar^{7+} and Ar^{8+}, using 1 ps pulses at 1053 nm, have been given to be about 2×10^{16} W/cm^2 and close to 3×10^{16} W/cm^2, respectively.[29,30] The intensity in the present work turns out to be higher (4×10^{16} W/cm^2), but this discrepancy could be attributed to other experimental reasons (different laser system, ion transmission, etc.).

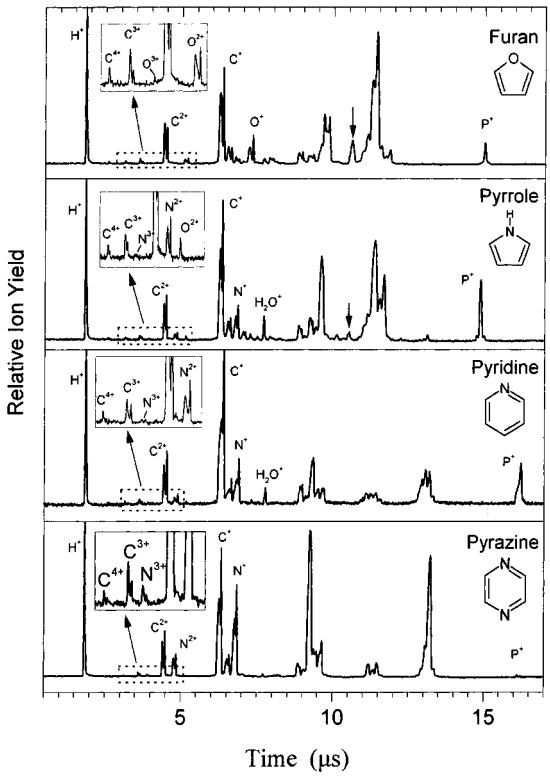

Figure 1. The mass spectra of furan, pyrrole, pyridine and pyrazine recorded at $I = 4 \times 10^{16}$ W/cm^2 ($\lambda = 790$ nm). The parent ions are denoted by a P while the doubly charged parent ions by an arrow.

Results and Discussion

Figure 1 shows the mass spectra recorded for the examined aromatic molecules at $\lambda = 790$ nm and $I = 4 \times 10^{16}$ W/cm^2. The abundance of the parent ions was found to be smaller compared to that reported previously using lower laser intensities.[26] This observation leads to the conclusion that the parent ions are unstable at these intensities. Their appearance at the mass spectra at higher intensities (4×10^{16} W/cm^2) should be attributed to ionization processes at the outer region of the focal area, where the laser intensity is significantly lower. In the mass spectra of furan and pyrrole the ion peaks denoted by an arrow have been assigned to doubly charged parent ions (P^{2+}). These peaks are broad. This broadening is possible attributed to metastable dissociation processes in these ions during the flight toward the ion detector.

Of particular interest are the peak profiles of the ions corresponding to light molecular fragments and atomic ions. These peaks exhibit a sharp and a broad component. These profiles could be attributed to space charge effects.[29] Nevertheless, this explanation is excluded on the ground of the following experimental observations:

- these peak profiles have been observed also at very low gas pressures ($<10^{-6}$ Torr)
- there is a systematic dependence of these profiles on laser intensity
- the absence of this type of profile for the H_2O^+ peak (Figure 2) even at the higher laser intensities used (water exists in the chamber as a contamination).

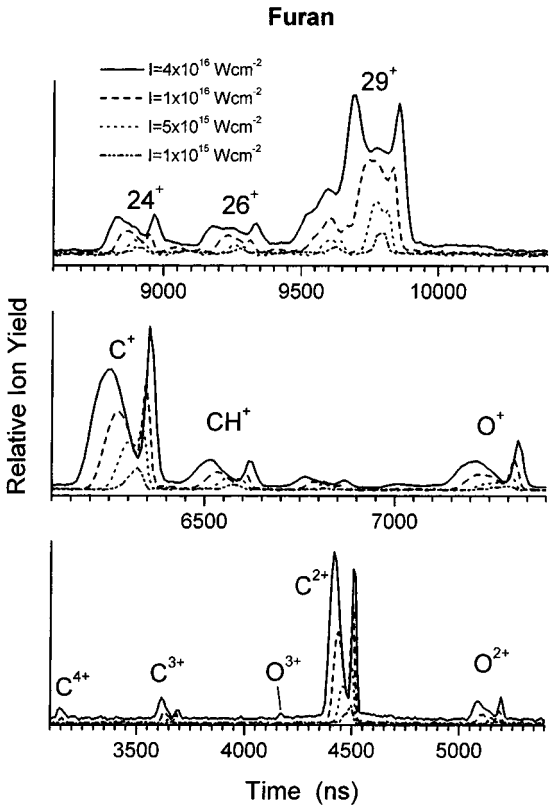

Figure 2. The light mass molecular fragments region of the mass spectra of furan, recorded at four different laser intensities.

Thus, these peak shapes are spectral features carrying information about the dissociation processes taking place in the molecular systems. It is worth noting that similar peak profiles have been reported previously.[31,32]

In Figure 2 the mass spectra of some light fragments of furan, recorded at different laser intensities, are shown. It is clear that at 10^{15} W/cm^2 no splitting of the peaks is observed while the splitting between the sharp and broad components increases with laser intensity. The same dependence on the laser intensity was observed in all ionic fragments of the molecules studied in the present work.

The peak shape can be explained by assigning the two components to the fragments ejected in back and forward (with respect to the TOF axis) directions. Specifically, for laser intensities higher than 10^{15} W/cm^2, multiply charged transient species are produced followed by an explosion resulting in the production of stable ions with high kinetic energies. Fragments with the same mass are generated through explosion of different transient multiply charged species, generating thus ions with a broad kinetic energy distribution. This broad distribution is reflected in the broad profile of one of the mass peak components, which as shown below corresponds to ions ejected in the forward direction. In contrast, the backward ejected ions produce a sharp peak because of the influence of the extraction field used. The laser intensity value of 10^{15} W/cm^2 can be considered as a threshold for these processes, since no splitting or broadening has been observed at this intensity level with the experimental set up used for the molecules under study.

To check the above interpretation of the mass peak profiles, a computer simulation of the ion trajectories has been made for the specific geometry and the extraction field used in the present experiment. In Figure 3 the results for the case of C^+ ion are shown. It is assumed that the C^+ ions are produced in two directions (forward and backward) with the same kinetic energy distribution, in the 0−60 eV range. The ion abundance, at discrete energies, has been fitted by a Gaussian in order to aid the eye of reader. The expected arrival times on the detector for C^+ ions with different initial kinetic energies are denoted on the figure. The simulated peak profile has two components and resembles closely the experimental one. The only difference is in the experimental peak profile where the areas of the sharp and the broad components are not equal. The sharp peak area is smaller than expected, because some of the ions ejected backward miss the detector. Thus, by measuring the peak separation (splitting) and the tail of the broad component in these profiles, it is possible to gain further insight on the processes taking place in the dissociation of molecular systems under strong laser field irradiation.[33] The relation connecting

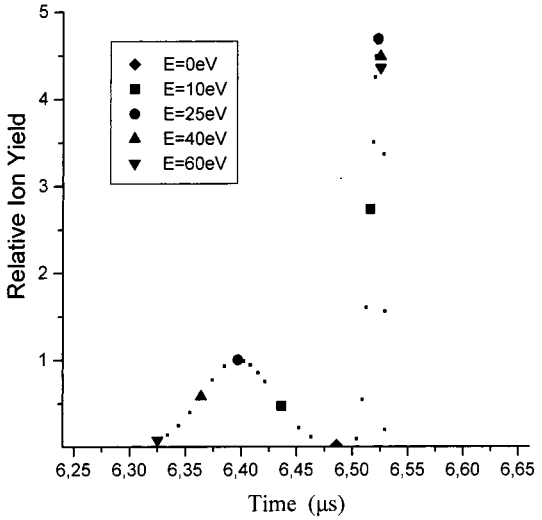

Figure 3. The peak profile of C^+ ion produced by a computer simulation. It is assumed that the ions are ejected in backward and forward directions with a kinetic energy distribution in the 0−60 eV range. Different symbols have been used to denote ions with specific kinetic energies.

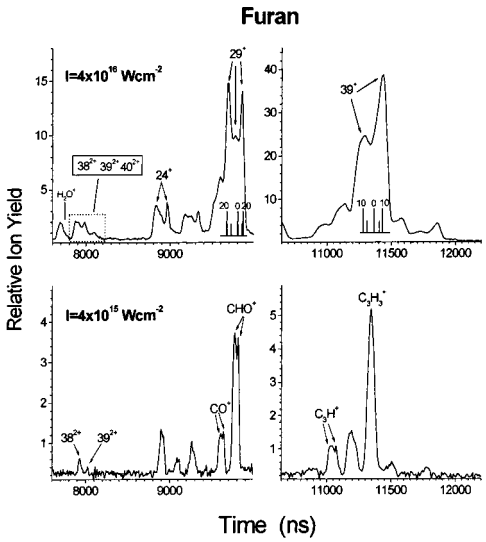

Figure 4. The region of the mass spectra of furan close to $m/z = 29$ and $m/z = 39$ ions are shown. The mass spectra have been recorded at laser intensities of $I = 4 \times 10^{16}$ W/cm^2 and 4×10^{15} W/cm^2. The asymmetric shape of the mass peak $m/z = 39$ at $I = 4 \times 10^{16}$ W/cm^2 is attributed to the contribution from parts of the $m/z = 38$ and $m/z = 40$ ion peaks. The scales alongside are the kinetic energy releases in eV.

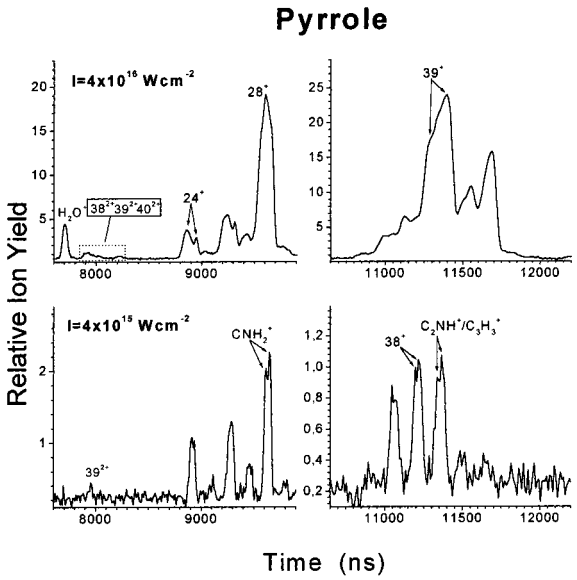

Figure 5. The region of the mass spectra of pyrrole close to the $m/z = 28$ and $m/z = 39$ ions are presented. The asymmetric shape of the mass peak $m/z = 39$ at $I = 4 \times 10^{16}$ W/cm^2 is attributed to the contribution from parts of the $m/z = 38$ and $m/z = 40$ ion peaks.

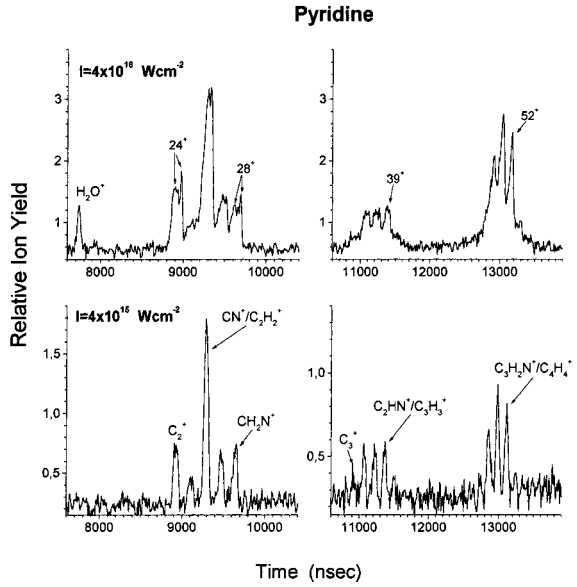

Figure 6. The light mass molecular fragments region of the mass spectra of pyridine recorded at laser intensities of $I = 4 \times 10^{16}$ W/cm^2 and 4×10^{15} W/cm^2.

the splitting of the ion peaks and the kinetic energy is

$$E(\text{eV}) = 9.65 \times 10^{-7} \frac{n^2 \Delta t^2 F^2}{8m} \qquad (1)$$

where n is the charged state, Δt (ns) is the time difference between the backward and forward ions, F(V/cm) is the extraction field, and m is the ion mass. Thus, the splitting Δt gives the kinetic energy of the majority of the fragments, while the shorter arrival time tail of the broad component corresponds to the highest kinetic energy available for the fragments. In the present work the kinetic energies of the fragment ions have been calculated also by computer simulation of their trajectories in the TOF system. The calibration of the system is based on the parent ion position as well as on ion peaks that have been recorded without the above-mentioned splitting (low laser intensity case). The kinetic energy values found to be similar, within the experimental error, with those calculated using eq 1.

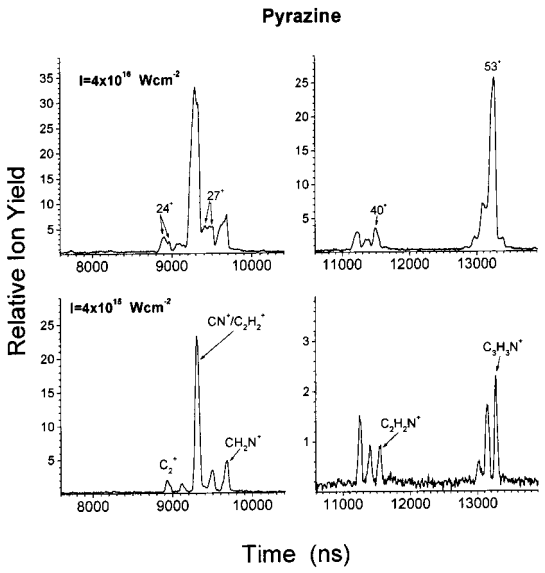

Figure 7. The light mass molecular fragments region of the mass spectra from pyrazine recorded at laser intensities of $I = 4 \times 10^{16}$ W/cm^2 and 4×10^{15} W/cm^2.

Molecular Fragments. Figures 4−7 show the mass spectral range corresponding to the molecular fragments recorded at laser intensities 4×10^{15} and 4×10^{16} W/cm^2 for all molecules studied. The observed molecular fragments are the same with those reported using electron impact mass spectrometry.[34] At 4×10^{15} W/cm^2, splitting of the fragment ions is clearly observed for furan (Figure 4) and pyrrole (Figure 5), but it is much less pronounced for pyridine (Figure 6) and pyrazine (Figure 7). In the case of the former molecules, kinetic energies, estimated from the observed splitting, are found to be in the range of 1−1.5 eV for all molecular fragments. Fragments with such kinetic energies suggest the involvement of a charge separation process.[35−38] This is further consistent with the observation of stable doubly charged parent ions (P^{2+}) and doubly charged molecular fragments [$m/z = 19$ ($C_3H_2^{2+}$), $m/z = 19{,}5$ ($C_3H_3^{2+}$) for furan and $m/z = 19{,}5$ ($C_3H_2^{2+}$) for pyrrole] for these two molecules. A typical charge separation processes could take place through the following steps:

$$P^{2+} \rightarrow F_1^{+} + F_2^{+}$$

$$P^{n+} \rightarrow F_1^{n_1+} + F_2^{n_2+} \; (n = n_1 + n_2)$$

Assuming a two charged points system, the repulsive potential is converted into kinetic energy of the products during the dissociation process. The assumption of point charges is inadequate and a charge distribution should be used. Nevertheless, it can provide a first-order semiquantitative approximation and it has been used before for pyridine and related systems such as benzene.[35] The total Coulomb repulsion energy (E_{tot}) can be estimate through

$$E_{\text{tot}}(\text{eV}) = \frac{14.4 n_1 n_2}{r(\text{Å})} \qquad (2)$$

where r is the distance between the two charges and $n_{1,2}$ is the charge of the fragments. Furthermore, the relation between E_{tot}

TABLE 1: The Estimated Kinetic Energies for the Molecular Fragments at $I = 4 \times 10^{16}$ W/cm^2

furan		pyrrole	
m/*z*	energy (eV)	*m*/*z*	energy (eV)
39^+	8 ± 1.5	39^+	6 ± 1
(29^+, 26^+, 24^+)	(16, 17, 13) $\pm$ 2	(28^+, 26^+, 24^+)	9 ± 2
pyridine		**pyrazine**	
m/*z*	energy (eV)	*m*/*z*	energy (eV)
(39^+, 38^+, 37^+)	3 ± 0.5	(40^+, 39^+, 38^+)	2 ± 0.5
(28^+- 24^+)	5 ± 1	(28^+− 24^+)	5 ± 1

and the final kinetic energy E_i of a fragment is

$$E_i = E_{tot}\left(1 - \frac{m_i}{M}\right) \quad (3)$$

where M is the mass of the precursor ion and m_i is the ion mass. As mentioned above, the parent ions P^{2+} have been observed only for furan and pyrrole. If a charge separation process is taking place in these two molecules and the dissociation channels are the same with those found for singly charged ions,[33,39,40] the following main reactions are expected to be valid:

furan

$$C_4H_4O^{2+} \rightarrow C_3H_3^+ + CHO^+$$
$$C_3H_4^+ + CO^+$$

pyrrole

$$C_4NH_5^{2+} \rightarrow C_2NH_3^+ + C_2H_2^+$$
$$C_3H_3^+ + CH_2N^+$$

From the splitting of the mass peaks, the kinetic energy is estimated to be $E_{tot} = 2-3$ eV, corresponding to an intercharge distance r (eq 2) of 5−7 Å. This distance is significantly larger than the diameter of the cyclic structure of furan and pyrrole and leads to the assumption of a deformed structure for the doubly charged molecular parent ion.

Furthermore, when more than two point charges are assumed in the precursor, E_{tot} is given by the equation

$$E_{tot}[(\mathbf{R}_i)_{i=1,n}] = \sum_{i<j} \frac{Z_i Z_j}{|\mathbf{R}_j - \mathbf{R}_i|}$$

where $(\mathbf{R}_i)_{i=1,n}$ represent the vector positions of the n repelling ions. These energy values are related to the initial positions of the repelling ions in the transient molecular species, since the kinetic energy of the precursor is negligible compared to Coulomb repulsion energy. The determination of the kinetic energy of each ion, after Coulomb explosion, is achieved by solving the coupled equations of motion.[7−9]

The splitting between the two components in each mass peak is found to be larger at higher laser intensity 4×10^{16} W/cm^2 (Figures 4−7). The estimated kinetic energies of the fragments at this intensity are given in Table 1. Such large energy values cannot be attributed to the Coulomb repulsion between only two charged fragment ions, produced in a $P^{3+} \rightarrow F_1^+ + F_2^{2+}$ type reaction, because the required separation distances (eq 2) must be smaller than the bond length. Therefore, it is reasonable to assume that at these laser intensities, the ionic fragments are produced by dissociation of higher charged parent ions (P^{n+}, $n>3$). Such processes could be direct (instantaneous) or sequential.

For the molecular fragment ions the broad component is not as extended as for the lighter mass ions (atomic), which implies that they are produced with lower kinetic energies. This indicates that the molecular fragment ions are generated through Coulomb explosion of transient species in lower charged states compared to those in which the explosion leads to highly energetic atomic ions.

The kinetic energies of the molecular fragments from furan and pyrrole were found to be higher than those from pyridine and pyrazine (Table 1).

To interpret the high kinetic energy found, for instance, for the $m/z = 29$ (CHO^+) ion peak in the mass spectra of furan, the maximum kinetic energy which can be reached by this ion is theoretically determined, by assuming that this is produced, as it is believed, through the dissociation of the [P^{4+}] transient parent ion state according to the scheme: [P^{4+}] → $CH^+ + CH^+ + CH^+ + CHO^+$.

The [P^{4+}] must be the maximum charged transient state of the parent ion leading to CHO^+ production, since for higher charged states ($n \geq 5$) fragmentation of the CHO^+ ion and/or the production of doubly charged fragments is expected. The [P^{4+}] of furan can fragment through a sequential or a direct mechanism from a cyclic or a deformed structure induced by the laser field. Obviously, the maximum kinetic energy for the CHO^+ fragment can be reached, if this ion is produced through a direct dissociation of [P^{4+}] from a linear structure, with CHO^+ being at the end of this configuration. In this case, by solving the coupled equations of motion, the estimated maximum kinetic energy for CHO^+ is ∼17 eV, if a charge distance of $r = 1.5$ Å is assumed, and ∼13 eV for $r = 1.8$ Å. These r values are longer than the bond length at the ground state of the neutral molecule ($r = 1.38$ Å).[41] On the contrary, explosion of a cyclic (aromatic) configuration of [P^{4+}], through symmetric charge separation, gives a maximum kinetic energy for CHO^+ of about 13 eV, even for $r = 1.38$ Å.

The peak splitting for CHO^+ (Table 1), at $I = 4 \times 10^{16}$ W/cm^2, corresponds to a kinetic energy of 16 ± 2 eV which seems to support a direct dissociation mechanism from a deformed configuration. Similarly, the corresponding energy from the peak splitting of the CH^+ ion, at the same laser intensities, is found to be 28 ± 4 eV, while theoretically is estimated to be 21 eV, for $r = 1.5$ Å. The slightly higher measured kinetic energies should be attributed to the contribution from CH^+ ions produced through explosions in higher charged states ($n \geq 5$).

As mentioned above the deformed molecular structure for the doubly charged parent ion is supported from the analysis made for the lower laser intensities used. The same conclusion seems to be supported also for the transient multiply charged parent ions. The only difference is the charge separation distance, which is significantly shorter at the higher charged transient parent ions.

These differences in the r values for doubly and multiply charged parent ions cannot be understood, if a stepwise ionization mechanism was involved. Thus, a consequence of the above analysis is that, at least for furan, the multiply molecular ionization process is achieved through a direct field ionization mechanism. This is in agreement with the work reported for smaller molecules,[42] but to our knowledge, it is verified for the first time in aromatic molecular systems like furan.

As far as the other molecules are concerned, it seems that for pyrrole the ionization/dissociation mechanisms are similar

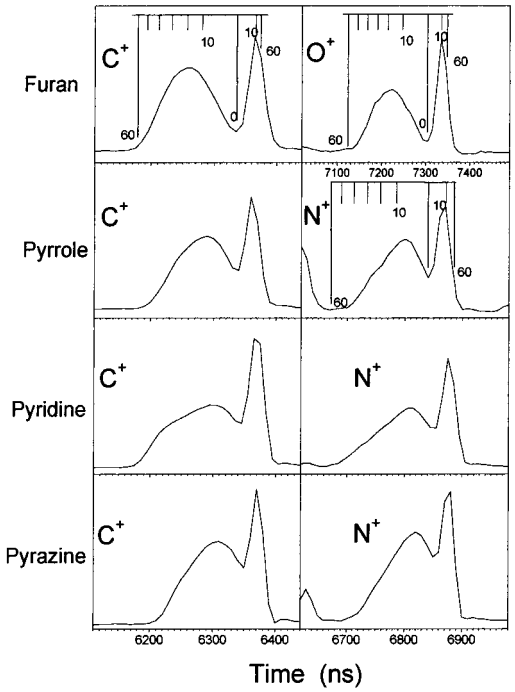

Figure 8. The peak profiles of the singly charged atomic ions from furan, pyrrole, pyridine and pyrazine, recorded at $I = 4 \times 10^{16}$ W/cm^2. The scales alongside are the kinetic energy releases in eV.

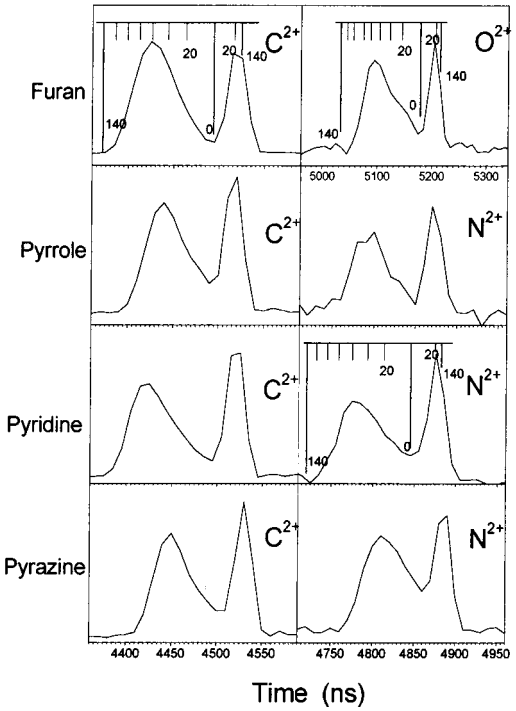

Figure 9. The peak profiles of the doubly charged atomic ions from furan, pyrrole, pyridine and pyrazine recorded at $I = 4 \times 10^{16}$ W/cm^2. The scales alongside are the kinetic energy releases in eV.

to those of furan. These two molecules have also some other common characteristics: their P^{2+} ion peak is pronounced in the recorded mass spectra and both have a five member aromatic ring.

On the other hand, the corresponding kinetic energies to molecular fragments of pyridine and pyrazine are smaller. This indicates that these molecules do not reach the same charged states as furan and pyrrole or if they do, their dissociation proceeds sequentially.

Multicharged Atomic Fragments. A common feature of the mass spectra shown in Figure 1 is the appearance of multiply charged atomic ions (C^{Z+}, N^{Y+}, O^{Y+}, where $Z = 1-4$ and $Y = 1-3$). These are expected to be generated at the spatial 'hottest' point of the laser focal area. The strong contribution of the multiply charged atomic ions in the total ion signal implies that a Coulomb explosion, in highly charged transient species, is the main dissociation process at these laser intensities.

Figures 8−10 show the mass spectra of the multicharged atomic ions, at $I = 4 \times 10^{16}$ W/cm^2. The atomic ions have peak profiles similar to those of molecular fragment ions. Once again, based on these profiles, two kinds of kinetic energies have been estimated. The first one is based on the arrival time of the maximum of the broad component and corresponds to the kinetic energies of the majority of the fragments at these laser intensities. The second value for the kinetic energy is based on the shorter time tail of the broad peak and has to do with the most energetic fragments (Table 2).

The peak profiles of singly charged atomic ions are presented in Figure 8. It is clear that the broad component does not have the same shape for all molecules. It is symmetric for furan but asymmetric for the other molecules. Furthermore, the kinetic energies, which correspond to the maximum of the broad component, are lower especially for pyridine and pyrazine. The asymmetry of the broad peak is believed to come from the convolution of different processes, which lead to singly charged atomic ion production. The calculated kinetic energies imply that the majority of these ions are generated with relatively smaller kinetic energies. Therefore, the asymmetry of the broad component reflects also a wider contribution of singly charged atomic ions derived from different processes. The fact that the kinetic energies are small could be evidence that these formation processes are sequential and/or that the majority of the molecules do not reach the same charged state as furan.

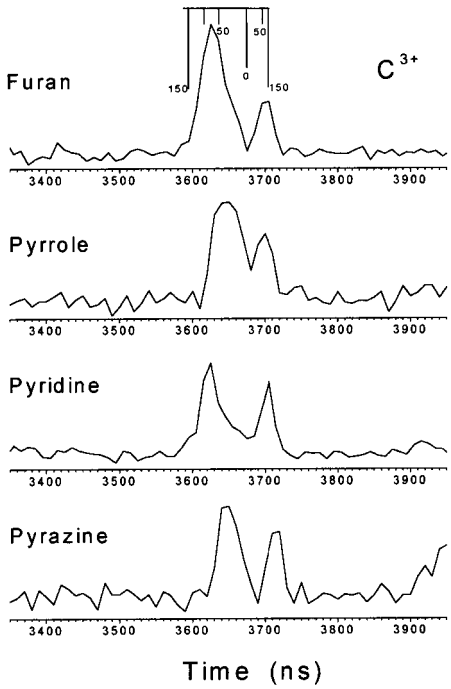

Figure 10. The peak profiles of triply charged carbon ions from furan, pyrrole, pyridine and pyrazine recorded at $I = 4 \times 10^{16}$ W/cm^2. The scale alongside are the kinetic energy releases in eV.

On the contrary, the peak shapes of the singly charged atomic fragments from furan are consistent with the interpretation made above, i.e., a direct Coulomb explosion, of highly charged transient species takes place in this molecule.

TABLE 2: The Calculated Kinetic Energies of the Multiply Charged Atomic Ions Based on (a) the Arrival Time of the Maximum and (b) the Short Time Tail of the Broad Component

	energy (eV)				
	(a)			(b)	
	C^+	C^{2+}	C^{3+}	C^+	C^{2+}
furan	20 ± 4	60 ± 13	75 ± 15	58 ± 6	125 ± 19
pyrrole	10 ± 2	41 ± 10	70 ± 14	55 ± 6	108 ± 17
pyridine	8 ± 2	60 ± 13	85 ± 15	67 ± 6	125 ± 19
pyrazine	8 ± 2	35 ± 10	75 ± 15	50 ± 5	85 ± 15
	A = N, O				
	A^+	A^{2+}	A^+	A^{2+}	
furan	17 ± 4	65 ± 13	54 ± 6	125 ± 15	
pyrrole	8 ± 2	43 ± 10	45 ± 6	95 ± 14	
pyridine	7 ± 2	55 ± 13	55 ± 6	125 ± 15	
pyrazine	7 ± 2	35 ± 10	40 ± 5	85 ± 13	

The peak profiles of doubly and triply charged atomic ions are shown in Figures 9 and 10 ($I = 4 \times 10^{16}$ W/cm^2). The estimated kinetic energies for the multicharged atomic ions (A^{n+} where A = C, N, O and $n>1$) are presented in Table 2. These values are much higher than those of the molecular fragment ions (Table 1), and therefore it is reasonable to assume that when the dissociation leads to multiply charged atomic ions, the direct Coulomb explosion mechanism is dominant in high multicharged transient species. It is worth noting that Shimizu et al. have recently reported such high kinetic energies for atomic multiple charged ions produced through Coulomb explosion in benzene.[43]

Finally, to check the influence of the molecular configuration on the atomic ion production, the abundance ratio (C^{Z+}/A^{Z+} where A = N, O and $Z = 1-3$) have been measured at laser intensities 4×10^{16} W/cm^2 (Figure 11a,b,c). The abundance ratio for singly charged atomic ions (C^+/A^+, A = N, O) turns out to be almost equal to the ratio of the atoms in the molecular skeleton (C/A, A = N, O) for all molecules studied in this work. The slight divergence of the ratio (C^+/N^+) from the stoichiometric ratio is attributed to the contribution in the $m/z = 14$ ion peak intensity of the CH_2^+ fragments. In absolute values, the ion yield of the singly charged atomic ions (Figure 11b) was found to be equal for all molecules having the same number of the specific atom in their molecular skeleton. In other words, the recorded C^+ ion abundance is similar for furan, pyrrole and pyrazine (all have four C atoms in their skeleton) and the same holds for N^+ ions in pyrrole and pyridine. Thus, it seems that the efficiency of the singly charged atomic ion production is independent of the atomic environment within the molecule.

The equality between the abundance ratios and the stoichiometric ratio is not preserved for all multiply charged atomic ions. Although the ratios of doubly (C^{2+}/N^{2+}) and triply (C^{3+}/N^{3+}) charged atomic ions in pyrazine and pyridine is found to be equal to the stoichiometric ratios, for furan (C^{Z+}/O^{Z+}, $Z = 2, 3$) and pyrrole (C^{Z+}/N^{Z+}, $Z = 2, 3$), the observed ratios turn out to be larger (Figure 11a). This difference in furan and pyrrole implies that the detection of multiply charged carbon atoms is more efficient in these two molecules (Figure 11b,c). It is interesting to note that the $C^{2,3+}$ ion yield is higher in furan from that recorded for pyridine, which has five carbons in the ring. The explanation for these observations is not obvious and may be related to the geometry of the multiply charged transient species within which the explosion takes place. In general, Coulomb explosion in a cyclic molecular configuration is expected to result in an isotropic distribution (in all directions) of the ejected fragments. Some of these ions could miss the ion detector since the multiply charged atomic ions are formed with high kinetic energies. In contrast, explosion from a linear (or close to linear) molecular structure, oriented by the laser field (which is horizontally polarized), is probable to result in more efficient multiple charged atomic ion detection. Within this approach there is a problem concerning the time scale needed for these structural changes with respect to the laser pulse duration. Very recently Fuss et al. have calculated that the photochemical ring opening of 1,3-cyclohexadiene could take place within 200 fs, while the time constant for the isomerization to tZt conformer (almost linear structure) found to be 580 ± 60 fs.[44] Their work has shown that the strong laser field does not automatically stretch the molecule during multiple ionization. For the molecules studied in the present work such data are not available. Undoubtedly, further experimental investigation is needed in order to explain the above observations.

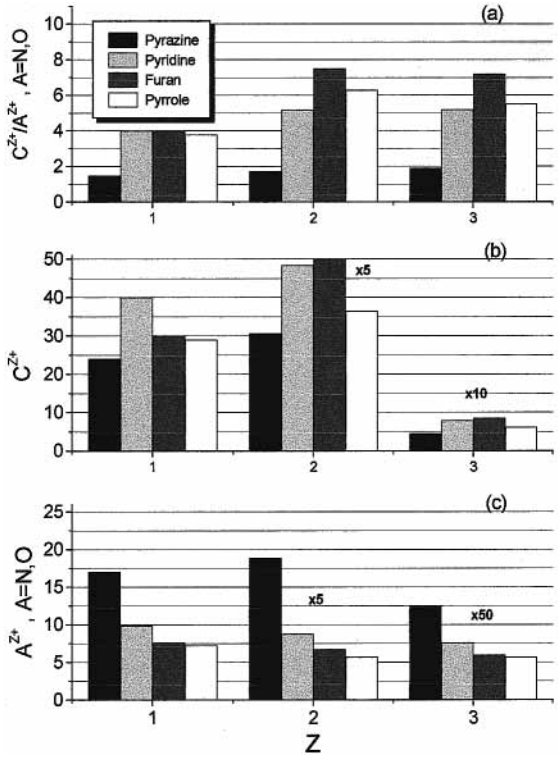

Figure 11. (a) The abundance ratios of multiply charged atomic ions (C^{Z+}/A^{Z+}, A = N, O and $Z = 1-3$) for the molecules studied. In (b) and (c) the ion yields of C^{Z+} ($Z = 1-3$), and A^{Z+} (A = N, O and $Z = 1-3$) are presented in arbitrary units ($I = 4 \times 10^{16}$ W/cm^2).

Conclusions

The fragmentation processes of multiply charged transient states of aromatic molecules induced by strong laser pulses (4×10^{16} W/cm^2) has been studied at $\lambda = 790$ nm. Because of the extraction field used, the generated through Coulomb explosion ions exhibit a structure which is consisting of one broad and one sharp component.

At a laser intensity of 4×10^{15} W/cm^2 there is evidence that the doubly charged parent ions of furan is fragmented from deformed molecular structure through a charge separation process. At higher laser intensities, the fragment ions seem to have been produced through Coulomb explosion of even higher charged parent ions (P^{n+}, $n \geq 3$). The molecular fragment ions are produced with lower kinetic energies than the lighter ionic masses (atomic). The former ions are generated through Coulomb explosion within transient species in lower charge state

compared to those in which the explosion leads to highly energetic atomic ions. In the case of furan the dissociation of the multiply charged transient parent ion [P^{4+}] seems to be a direct one. Moreover, the estimated charge separation distances support a direct field ionization mechanism for this molecule.

The kinetic energies of the molecular fragment ions were found to be smaller in the case of pyridine and pyrazine than in furan and pyrrole. It seems that pyridine and pyrazine do not reach the same charged states as furan and pyrrole or, if they do, their dissociation proceeds sequentially.

The multiply charged atomic ions (C^{Z+}, N^{Y+}, O^{Y+}, $Z = 1-4$ and $Y = 1-3$) are the main products at 4×10^{16} W/cm^2 laser intensity. Their dominance demonstrates that the produced highly charged molecular species dissociate through Coulomb explosion.

It turns out that the multiply charged atomic ions (C^{Z+}, N^{Y+}, O^{Y+}, $Z = 2-4$ and $Y = 2-3$) are generated through a direct Coulomb explosion of multiply charged transient parent ions, for all the molecules studied.

The efficiency of the singly charged atomic ion production was found to be independent of the atomic environment within the molecule and the abundance ratios (C^+/A^+, A = N,O) are equal to the stoichiometric ratios in the molecule. The equality between the abundance ratios and the stoichiometric ratios was not found to be preserved for the multiply charged atomic ions in the case of furan and pyrrole.

Acknowledgment. We would like to express our thanks to the Rutherford Appleton Laboratory for their excellent facilities and their assistance. P.G. would like to thank EPSRC for financial support.

References and Notes

(1) Frasinski, L. J.; Codling, K.; Hartherly, P.; Barr, J.; Ross, I. N.; Toner, W. T. *Phys. Rev. Lett.* **1987**, *58*, 2424.
(2) Codling, K.; Frasinski, L. J. *J. Phys. B* **1993**, *26*, 783.
(3) Seideman, T.; Ivanov, M. Y.; Corkum, P. B. *Phys. Rev. Lett.* **1995**, *75*, 2819.
(4) Villeneuve, D. M.; Ivanov, M. Y.; Corkum, P. B. *Phys. Rev. A* **1996**, *54*, 736.
(5) Constant, E.; Stapelfeldt, H.; Corkum, P. B. *Phys. Rev. Lett.* **1996**, *76*, 4140.
(6) Schmidt, M.; Normand, D.; Cornaggia, C. *Phys. Rev. A* **1994**, *50*, 5037.
(7) Cornaggia, C.; Schmidt, M.; Normand, D. *Phys. Rev. A* **1995**, *51*, 1431.
(8) Cornaggia, C. *Phys. Rev. A* **1995**, *52*, R4328.
(9) Cornaggia, C. *Phys. Rev. A* **1996**, *54*, R2555.
(10) Hering, P.; Cornaggia, C. *Phys. Rev. A* **1998**, *57*, 4572.
(11) Keldysh, L. V. *Sov. Phys. JETP* **1965**, *20*, 1307.
(12) Levis, R. J.; DeWitt, M. J. *J. Phys. Chem. A* **1999**, *103*, 6493.
(13) DeWitt, M. J.; Levis, R. J. *Phys. Rev. Lett.* **1998**, *81*, 5101.
(14) DeWitt, M. J.; Levis, R. J. *J. Chem. Phys.* **1995**, *102*, 8670.
(15) DeWitt, M. J.; Levis, R. J. *J. Chem. Phys.* **1998**, *108*, 7045.
(16) DeWitt, M. J.; Levis, R. J. *J. Chem. Phys.* **1998**, *108*, 7739.
(17) Castillejo, M.; Couris, S.; Koudoumas, E.; Martin, M. *Chem. Phys. Lett.* **1998**, *289*, 303.
(18) Ledingham, K. W. D.; Kosmidis, C.; Georgiou, S.; Couris, S.; Singhal, R. P. *Chem. Phys. Lett.* **1995**, *247*, 555.
(19) Singhal, R. P.; Kilic, H. S.; Ledingham, K. W. D.; Kosmidis, C.; McCanny, T.; Langley, A. J.; Shaikh, W. *Chem. Phys. Lett.* **1996**, *253*, 108.
(20) Kilic, H. S.; Ledingham, K. W. D.; Kosmidis, C.; McCanny, T.; Singhal, R. P.; Wang, S. L.; Smith, D. J.; Langley, A. J.; Shaikh, W. *J. Phys. Chem. A* **1997**, *101*, 817.
(21) Kosmidis, C.; Ledingham, K. W. D.; Kilic, H. S.; McCanny, T.; Singhal, R. P.; Langley, A. J.; Shaikh, W. *J. Phys. Chem. A* **1997**, *101*, 2264.
(22) Ledingham, K. W. D.; Kilic, H. S.; Kosmidis, C.; Deas, R. M.; Marshall, A.; McCanny, T.; Singhal, R. P.; Langley, A. J.; Shaikh, W. *Rapid Commun. Mass Spectrom.* **1995**, *9*, 1522.
(23) Smith, D. J.; Ledingham, K. W. D.; Singhal, R. P.; Kilic, H. S.; McCanny, T.; Langley, A. J.; Taday, A. J.; Kosmidis, C. *Rapid Commun. Mass Spectrom.* **1998**, *12*, 813.
(24) Ledingham, K. W. D.; Smith, D. J.; Singhal, R. P.; McCanny, T.; Graham, P.; Kilic, H. S.; Peng, W. X.; Langley, A. J.; Taday, P. F.; Kosmidis, C. *J. Phys. Chem. A* **1999**, *103*, 2952.
(25) Smith, D. J.; Ledingham, K. W. D.; Singhal, R. P.; McCanny, T.; Graham, P.; Kilic, H. S.; Tzallas, P.; Kosmidis, C.; Langley, A. J.; Taday, P. F. *Rapid Commun. Mass Spectrom.* **1999**, *13*, 1390.
(26) Kosmidis, C.; Tzallas, P.; Ledingham, K. W. D.; McCanny, T.; Singhal, R. P.; Taday, P. F.; Langley, A. J. *J. Phys. Chem. A* **1999**, *103*, 6950.
(27) Smith, D. J.; Ledingham, K. W. D.; Kilic, H. S.; McCanny, T.; Peng, W. X.; Singhal, R. P.; Langley, A. J.; Taday, P. F.; Kosmidis, C. *J. Phys. Chem. A* **1998**, *102*, 2519.
(28) Taday, P. F.; Mohammeed, I.; Langley, A. J.; Ross, I. N.; Codling, K.; Ledingham, K. D. D.; Newell, W. R.; Preston, S.; Riley, D.; Williams, I. 1998 Central Laser Facility, RAL Annual Report 1997/98, 179.
(29) Auguste, T.; Monot, P.; Lompre, L. A.; Mainfray, G.; Manus, C. *J. Phys. B: At. Mol. Opt. Phys.* **1992**, *25*, 4181.
(30) August, S.; Meyerhofer, D.; Strickland, D.; Chin, S. L. *J. Opt. Soc. Am. B* **1991**, *8*, 858.
(31) Frasinski, L. J.; Codling, K.; Hatherly, P.; Barr, J.; Ross, N.; Toner, W. T. *Phys. Rev. Lett.* **1987**, *58*, 2424.
(32) Luk, T. S.; Moriarty, R. M.; Awashti, A.; Boyer, K.; Rhodes, C. K. *Phys. Rev. A* **1992**, *45*, 6744.
(33) Snyder, E. M.; Wei, S.; Purnell, J.; Buzza, S. A.; Castleman, A. W. *Chem. Phys. Lett.* **1996**, *248*, 1.
(34) *NIST Standard Reference Database 69*, November 1998 Release; NIST Chemistry Webbook; National Institute of Standards and Technology: Gaithersburg, MD 20899, 1998 (http://webbook.nist.gov/chemistry).
(35) Vekey, K. *Mass Spectrom. Rev.* **1995**, *14*, 195 and reference therein.
(36) Kingston, R. G.; Guilhaus, M.; Brenton, A. G.; Beynon, J. H. *Organic Mass Spectrom.* **1985**, *20*, 406.
(37) Leach, S.; Eland, J. H. D.; Price, S. D. *J. Phys. Chem.* **1989**, *93*, 7575.
(38) Nenner, I.; Eland, J. H. D. *Z. Phys. D*: *At., Mol. Clusters* **1992**, *25*, 47.
(39) Rennie, E. E.; Johnson, C. A. F.; Parker, J. E.; Holland, D. M. P.; Shaw, D. A.; MacDonald, M. A.; Hayes, M. A.; Shpinkova, L. G. *Chem. Phys.* **1998**, *236*, 365.
(40) Rennie, E. E.; Johnson, C. A. F.; Parker, J. E.; Ferguson, R.; Holland, D. M. P.; Shaw, D. A. *Chem. Phys.* **1999**, *250*, 217.
(41) Trofimov, A. B.; Koppel, H.; Schirmer, J. *J. Chem. Phys.* **1998**, *109*, 1025.
(42) Cornaggia, C.; Hering, Ph. *J. Phys. B* **1998**, *31*, L503.
(43) Shimizu, S.; Kou, J.; Kawato, S.; Shimizu, K.; Sakabe, S.; Nakashima, N. *Chem. Phys. Lett.* **2000**, *317*, 609.
(44) Fuss, W.; Schmid, W. E.; Trushin, S. A. *J. Chem. Phys*. **2000**, *112*, 8347.